Computers & Fluids 79 (2013) 134–139

Contents lists available at SciVerse ScienceDirect

Computers & Fluids

journal homepage: www.elsevier.com/locate/compfluid

Performance and implementation of the Launder–Sharma low-Reynolds number turbulence model

A. Mathur, S. He *

Department of Mechanical Engineering, University of Sheffield, Sheffield S1 3JD, UK

ARTICLE INFO

Article history:
Received 10 August 2012
Received in revised form 19 January 2013
Accepted 20 February 2013
Available online 14 March 2013

Keywords:
Turbulence model
Low-Reynolds number
FLUENT
Launder–Sharma

ABSTRACT

The Launder–Sharma model (Lett. Heat Mass Transfer 1, 1974, 131–138) is one of the earliest and most-widely used low-Reynolds number (LRN) models and has been shown to be in good agreement with experimental and DNS data for a range of turbulent flow problems, performing better than many other LRN k–ε models. However, some recent studies including those using commercial CFD solvers report the model to behave otherwise. In the present study, the LS model has been implemented in FLUENT using user-defined functions (UDFs), and its performance in predicting steady and unsteady turbulent flows has been tested and found to agree closely with those reported in the literature using 'in-house' CFD codes. However, this FLUENT-UDF LS model performs very differently from the in-built FLUENT LS model. The former agrees well with experimental and DNS data, whereas the latter does not. In addition, the UDF is used to demonstrate that the model predictions are very sensitive to the interpretation of the model formulation. Consequently, it is concluded that whereas the LS model is not sensitive to numerical method or method of coding, it is sensitive to changes in the interpretation of the formulation of the model.

1. Introduction

Eddy viscosity turbulence models are widely used because of their simplicity and broad applicability. Of these, two-equation models are most widely used and have gradually become industry-standard models. Such models use two transport equations to represent turbulent properties of the flow; e.g. turbulent kinetic energy, k, and turbulent dissipation, ε, or specific dissipation, ω. Launder and Spalding [1] proposed a k–ε turbulence model, where the turbulent shear stress is assumed to be related to the mean strain-rate via an *eddy viscosity*, which is determined by local values of density, turbulent kinetic energy and energy dissipation rate. This model is referred to as the *standard* k–ε model, and is used to simulate a variety of turbulent flows.

A challenge to turbulence modelling is that the direct application of the no-slip wall boundary condition to the model yields unsatisfactory results in the prediction of the flow near the wall. This is due to the presence of a very thin layer adjoining the wall where the eddy viscosity of the flow changes rapidly with distance from the wall, and its effect on the transport processes cannot be computed by an arithmetic- or harmonic-mean across this region. To overcome this shortcoming, a wall-function method is used by Launder and Spalding [1]. This approach bridges the viscous sublayer by employing empirical formulae in the region providing the boundary conditions to the mean-flow and turbulence equations. This circumvents the need to resolve the viscous sublayer with a fine mesh and solve the transport equations right up to the wall. The first grid node for this approach needs to lie outside the viscous sublayer. A typical requirement is $y_1^+ > 20$.

An alternative to the wall-function method is the low-Reynolds number (LRN hereafter) approach, where the transport equations are solved right up to the wall using a LRN model, which is developed to account for the near-wall phenomena. Jones and Launder proposed a LRN formulation in the 1972 paper [2], which was tested for shear flows in their 1973 paper [3]. The most widely used version of this model is the Launder–Sharma model [4] which uses the optimised model constants of Launder and Spalding [1].

Although the Launder–Sharma (LS hereafter) model was initially proposed for predicting swirling flows, it has been widely accepted a benchmark LRN k–ε formulation and used for a variety of turbulent flows in the literature. Comparative studies of different LRN models were done by Patel et al. [5] for boundary layer flows and by Betts and Dafa'Allah [6] for natural convection cavity flows. Both studies reported that LS model was one of only four LRN models that were in good agreement with experimental data. Similar studies were presented for turbulent pipe flow by Hrenya et al. [7,8] and Thakre and Joshi [9] in which the LS model performed reasonably well against DNS and experimental data. Cotton and Jackson [10] and Kim et al. [11] extended the study by testing its

* Corresponding author. Tel.: +44 114 2227756; fax: +44 114 2227890.
E-mail address: s.he@sheffield.ac.uk (S. He).

0045-7930/$ - see front matter © 2013 Elsevier Ltd. All rights reserved.
http://dx.doi.org/10.1016/j.compfluid.2013.02.020

performance for mixed convection air flow in vertical pipes and concluded that the model was in agreement with experiments in buoyancy-aided flows. He et al. [12] reported similar conclusions for mixed convection heat transfer to supercritical fluids.

The model is further proved to be able to predict unsteady turbulence as well. Jackson et al. [13] reported that LS model is able to reproduce transient response to heat transfer in turbulent pipe flow. Transient turbulence response has also been reported to be in good agreement with experiments by He and colleagues [14–17] for accelerating/decelerating pipe flows; and by Cotton and colleagues [18–21] for small-amplitude oscillating pipe flows.

In the above studies, the LS model had been implemented in '*in-house*' CFD codes, and had performed reasonably well in comparison with experimental and/or DNS data. However, recent reports using commercial CFD codes suggest otherwise. Wang and Majumdar [22] investigated the prediction of heat transfer for impingement jets using five LRN models available in the commercial CFD code FLUENT 6.1, and found that the LS model significantly overestimate the Nusselt number in the impinging region, performing worst among the models used. Similar results were reported by Du et al. [23] for heat transfer to supercritical CO_2 in vertical tubes, using the formulation available in FLUENT 6.2. Applicability of LRN models for flow past underwater hulls was investigated by Jagadeesh and Murali [24] with respect to surface pressure coefficient and pressure surface boundary layer. Four models implemented in FLUENT 6.1 were considered. Although all four models performed similarly, LS model showed most deviations from the experimental data.

A comparison of different CFD codes was discussed by Iaccarino [25], where the performance of LS model was investigated for a two-dimensional diffuser flow using three commercial codes – FLUENT 5.3, StarCD 3.1 and CFX 4.3. It was reported that even with the same computational grid and flow conditions, the three codes showed variations in velocity and turbulent kinetic energy profiles. A grid sensitivity analysis had also been performed to show that grid convergence had been reached in each code.

The difference in performance of the LS model discussed above is striking and is likely to be attributable to the way in which the model is implemented in the code. The purpose of this paper is to report an investigation into the effect of different implementations and/or interpretations of the model on the performance of the model in simulating a number of flows. In this study, we have implemented the LS model in FLUENT 12.1 using user-defined functions (UDFs) and compared its performance with that of the LS implemented in in-house CFD codes as well as that of the LS model inbuilt in FLUENT. We have then tested the sensitivity of different interpretations of the model formulation using the FLUENT-UDF approach and demonstrated that the effect is strong. The results have shown that whereas the model is rather robust and insensitive to numerical methods and method of coding used, its performance is highly sensitive to small changes in the formulation of the model.

2. The Launder–Sharma model

The Launder–Sharma LRN model [4], as a modified version of the standard k–ε model is one of the earliest and most widely used models for resolving the near-wall flow behaviour. The LS model differs from the standard model by the inclusion of damping functions in order to account for the viscous and wall effects. The model formulated for an unsteady axi-symmetric flow reads:

Constitution equation

$$-\overline{\rho u' v'} = \mu_t \frac{\partial u}{\partial r} \quad \text{where } \mu_t = \rho C_\mu f_\mu \frac{k^2}{\tilde{\varepsilon}} \tag{1}$$

Turbulent kinetic energy equation

$$\rho\frac{\partial k}{\partial t} + \rho\frac{\partial (Uk)}{\partial x} + \frac{1}{r}\rho\frac{\partial (rVk)}{\partial r} = \frac{\partial}{\partial x}\left[\left(\mu + \frac{\mu_t}{\sigma_k}\right)\frac{\partial k}{\partial x}\right] + \frac{1}{r}\frac{\partial}{\partial r}\left[r\left(\mu + \frac{\mu_t}{\sigma_k}\right)\frac{\partial k}{\partial r}\right] + P_k - \rho\varepsilon \tag{2}$$

Turbulent energy dissipation equation

$$\rho\frac{\partial \tilde{\varepsilon}}{\partial t} + \rho\frac{\partial (U\tilde{\varepsilon})}{\partial x} + \frac{1}{r}\rho\frac{\partial (rV\tilde{\varepsilon})}{\partial r} = \frac{\partial}{\partial x}\left[\left(\mu + \frac{\mu_t}{\sigma_\varepsilon}\right)\frac{\partial \tilde{\varepsilon}}{\partial x}\right] + \frac{1}{r}\frac{\partial}{\partial r}\left[r\left(\mu + \frac{\mu_t}{\sigma_\varepsilon}\right)\frac{\partial \tilde{\varepsilon}}{\partial r}\right] + C_1 f_1 \frac{\tilde{\varepsilon}}{k} P_k - C_2 f_2 \rho \frac{\tilde{\varepsilon}^2}{k} + E_\varepsilon \tag{3}$$

where $\tilde{\varepsilon} = (\varepsilon - D_\varepsilon)$.

$$P_k = \mu_t S^2 \tag{4}$$

where S is the strain-rate magnitude.

$$S = \sqrt{2S_{ij}S_{ij}} = \sqrt{\left[2\left\{\left(\frac{\partial U}{\partial x}\right)^2 + \left(\frac{\partial V}{\partial r}\right)^2 + \left(\frac{V}{r}\right)^2\right\} + \left(\frac{\partial U}{\partial r} + \frac{\partial V}{\partial x}\right)^2\right]} \tag{5}$$

The damping functions are

$$D_\varepsilon = 2\frac{\mu}{\rho}\left[\left(\frac{\partial \sqrt{k}}{\partial r}\right)^2 + \left(\frac{\partial \sqrt{k}}{\partial x}\right)^2\right],$$

$$E_\varepsilon = 2\frac{\mu\mu_t}{\rho}\left[\left(\frac{\partial S}{\partial r}\right)^2 + \left(\frac{\partial S}{\partial x}\right)^2\right], f_1 = 1.0,$$

$$f_2 = 1 - 0.3\exp(-Re_t^2), \quad f_\mu = exp\left[\frac{-3.4}{(1 + Re_t/50)^2}\right], \quad Re_t = \frac{\rho k^2}{\mu\tilde{\varepsilon}} \tag{6}$$

where C_1, C_2, C_μ, σ_k and σ_ε are empirical constants having the same value as in the standard k–ε model (i.e. 1.44, 1.92, 0.09, 1.0 and 1.3, respectively). f_1, f_2 and f_μ are damping functions to account for near-wall effects, and have the value unity far from the wall.

In the model, $\tilde{\varepsilon}(= \varepsilon - D_\varepsilon)$ is a modified dissipation rate of k, ε is the originally-defined dissipation rate, and D_ε a damping term. The reason for solving the $\tilde{\varepsilon}$ equation is purely computational as there are disadvantages in implementing the non-zero wall-boundary condition of ε. The transport equation of $\tilde{\varepsilon}$ is solved with a boundary value of zero at the wall, and the correct form of ε is recovered through $\varepsilon = (\tilde{\varepsilon} + D_\varepsilon)$ which is then used in the k transport equation. The value of D_ε is significant close to the wall but is negligible away from the wall. The final term in the dissipation equation, E_ε, has no physical significance. It is included to increase the predicted dissipation rate, and hence, to obtain realistic predictions of turbulent kinetic energy in the near-wall region.

The definition of E_ε given in Launder and Sharma [4] was formulated for a special case, namely, swirling axi-symmetric flows. The formulation in the present study (Eq. (6)) is an interpretation of that definition for an axi-symmetric flow, and will reduce to the original form for swirling flows.

3. Implementation of the LS model

As discussed earlier, an important feature of the LS model is that it uses a modified dissipation rate, $\tilde{\varepsilon}(= \varepsilon - D_\varepsilon)$. The difference between ε and $\tilde{\varepsilon}$ is small as their values are effectively the same

Table 1
Implementation cases in the present study.

Cases	Eddy viscosity (μ_t)	Turbulent Reynolds number (Re_t)
UDF-LS (Case A)	$\rho C_\mu f_\mu \frac{k^2}{\tilde{\varepsilon}}$ (*original*)	$\frac{k^2}{\nu\tilde{\varepsilon}}$ (*original*)
Case B	$\rho C_\mu f_\mu \frac{k^2}{\tilde{\varepsilon}+D_\varepsilon}$	*Original*
Case C	*Original*	$\frac{k^2}{\nu(\tilde{\varepsilon}+D_\varepsilon)}$
Case D	$\rho C_\mu f_\mu \frac{k^2}{\tilde{\varepsilon}+D_\varepsilon}$	$\frac{k^2}{\nu(\tilde{\varepsilon}+D_\varepsilon)}$

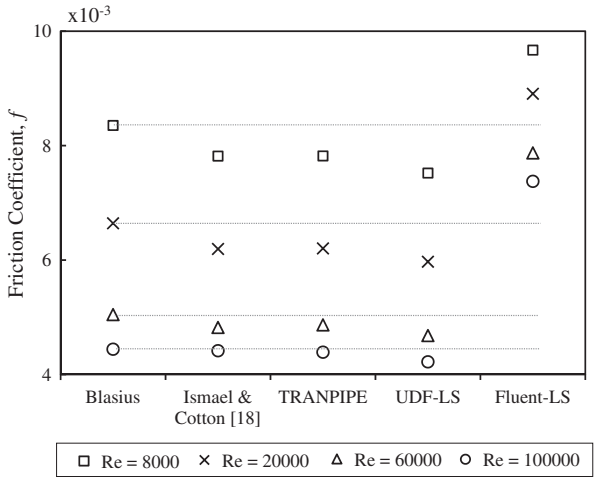

Fig. 1. Comparison of friction coefficient predicted using various CFD codes with Blasius correlation for a steady pipe flow.

for most part of the flow, and are different only in the region very close to the wall. As ε is replaced by $\tilde{\varepsilon}$ in the model only for numerical advantages, there is a question as which of these should be used in the definition of eddy viscosity (μ_t) and the turbulent Reynolds number (Re_t). The modified dissipation rate $\tilde{\varepsilon}$ is used in the original paper [4] but theoretically speaking, the original ε should be used. Several test cases have been designed to study the effect of these different interpretations.

The base case, referred to as Case A, is one where the definitions of μ_t and Re_t use the modified dissipation rate, $\tilde{\varepsilon}$, as given by the original paper, Launder and Sharma [4]. Table 1 lists the rest of the implemented cases used in the study. All cases are implemented in FLUENT 12.1 using user-defined functions (UDFs), which is documented in Online Resources of the Journal.

The LS model implemented in FLUENT 12.1 using UDFs is referred to as UDF-LS hereafter. The inbuilt viscous models in the CFD solver are turned off, and the turbulence parameters, k and $\tilde{\varepsilon}$ are solved as scalar quantities along with the momentum equations. The production and dissipation terms in these equations are added as 'scalar sources' to the transport equations, and the diffusivities of k and $\tilde{\varepsilon}$ are assigned accordingly. The eddy viscosity is computed from these scalar quantities and is added to the molecular viscosity for computing the *effective viscosity* of the momentum transport equations.

Apart from UDF-LS, two other implementations are also used. The first is the inbuilt low-Reynolds number LS model available in FLUENT 12.1 (referred to as Fluent-LS hereafter). The second model, referred to as TRANPIPE hereafter, is an in-house CFD code developed by the second author using FORTRAN specifically for modelling turbulent pipe flows. The model implemented is the same as that in UDF-LS, namely following the definitions of the

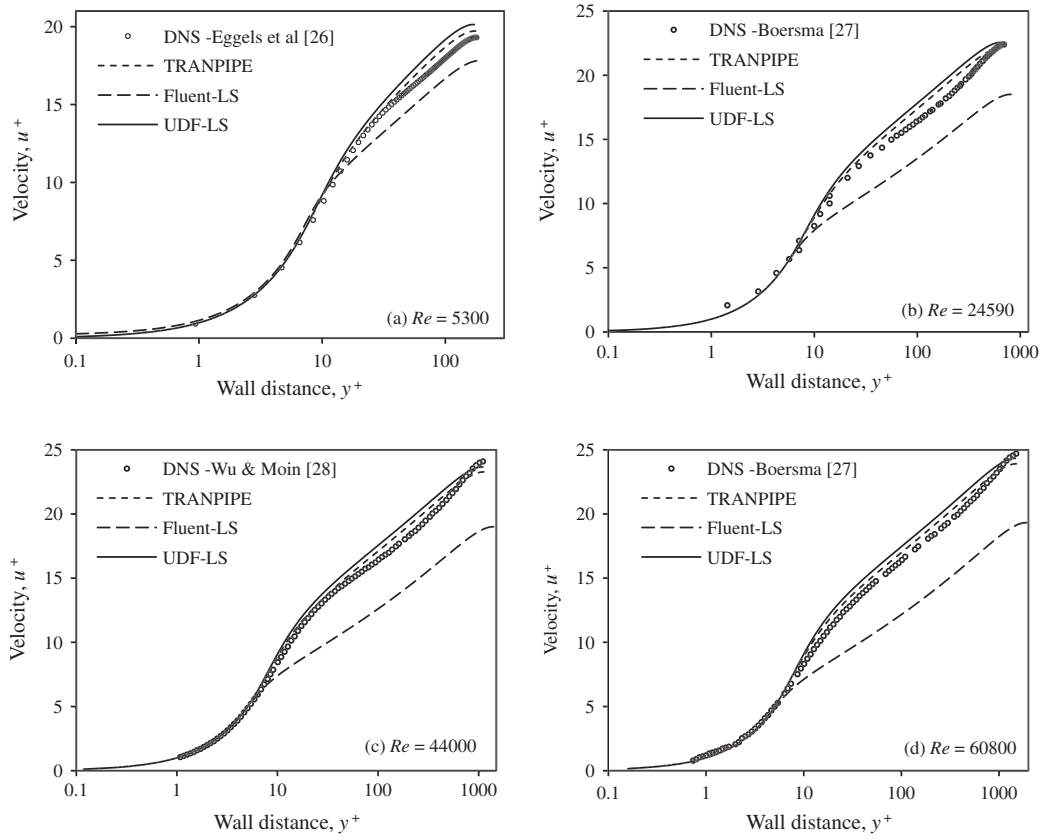

Fig. 2. Comparison of predictions using various CFD codes with DNS data for a steady pipe flow.

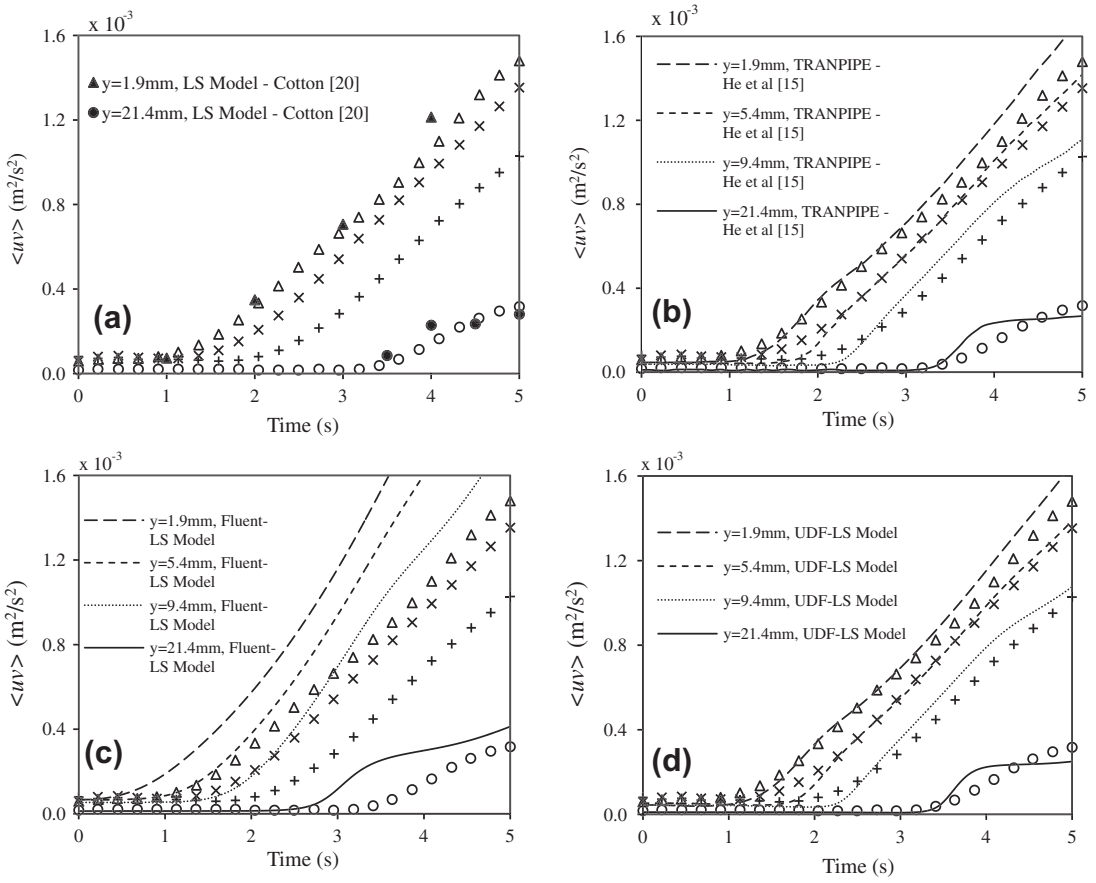

Fig. 3. Comparison of predictions using various CFD codes of an accelerating pipe flow from $Re_i = 7000$ to $Re_f = 45{,}000$ in 5 s. Experimental data points of He [14] – (Δ) $y = 1.9$ mm; (x) $y = 5.4$ mm; (+) $y = 9.4$ mm; (○) $y = 21.4$ mm.

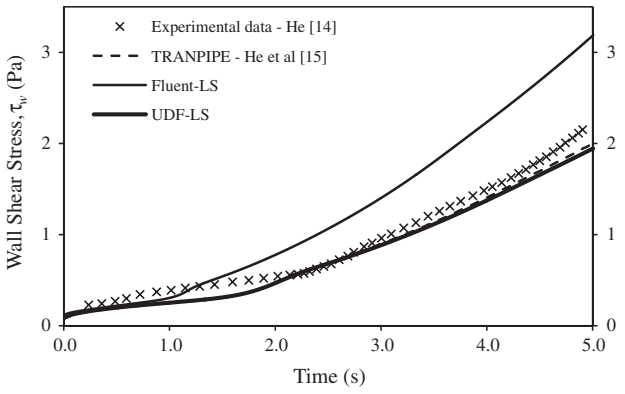

Fig. 4. Comparison of predictions of various CFD codes with experimental data of He [14] for an unsteady pipe flow.

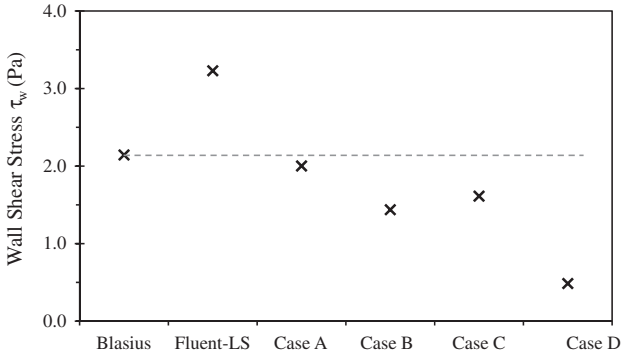

Fig. 5. Comparison of different LS model implementations for a steady pipe flow at $Re = 45{,}000$.

original paper [4]. This in-house code has been used and validated extensively over the years [11–17].

4. Results and discussion

4.1. Comparison of the LS model performance implemented in different CFD codes

The main objective of the study reported in this section is testing the sensitivity of the model performance to particular coding when the same version of the model (namely, the original [4]) is used. For this purpose, the UDF-LS and the TRANPIPE are used to reproduce and compare with some published simulations of the LS model. In addition, these simulations are compared with those using the inbuilt LS model in FLUENT 12.1.

Friction factors for steady pipe flow at four different Reynolds numbers are reported by Ismael and Cotton [18] using an in-house CFD code developed by the authors. These simulations are reproduced using three codes: UDF-LS, Fluent-LS and TRANPIPE, and along with the results reported by Ismael and Cotton, comparison is made with the Blasius prediction (i.e. $f = 0.079Re^{-0.25}$) (Fig. 1). For all Reynolds numbers, the results of Ismael and Cotton [18] and those of TRANPIPE are indistinguishable whereas those of UDF-LS are slightly lower but still very close to them. In contrast, Fluent-LS is found to predict a significantly higher friction

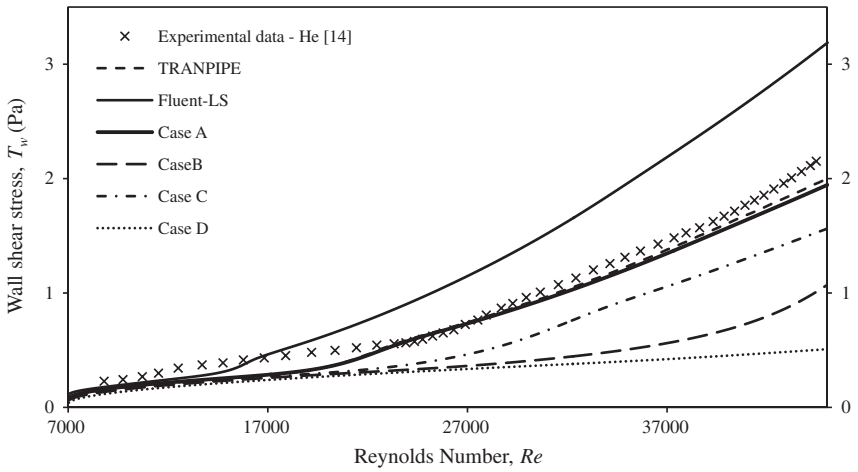

Fig. 6. Comparison of different LS model implementation for a 5 s ramp-up pipe flow.

coefficient in comparison with the other three codes. The discrepancies are larger for higher Reynolds numbers. It can also be seen that the Blasius correlation agrees well with the prediction of the first three codes for the two high Reynolds number cases but is somewhat lower than model predictions for low Reynolds number cases. It should be noted that the Blasius correlation is known to be unreliable for low Reynolds number flows. These results are included here for the sake of completeness.

Next, comparisons are made with DNS data with which detailed comparison on velocity profiles can be made. Four sets of turbulent pipe flow data were chosen to cover a range of Reynolds numbers: Re = 5300 by Eggels et al. [26], 24,590 and 60,800 by Boersma [27] and 44,000 by Wu and Moin [28]. Fig. 2a–d shows the comparison of the logarithmic velocity profile of the flow at the various Reynolds numbers. Again the prediction of UDF-LS and TRANPIPE agree well with each other for all Reynolds numbers and are close to the DNS data. In contrast, Fluent-LS's predictions are lower than the DNS data, with greater discrepancies at higher Reynolds numbers. A detailed inspection shows that the reason for this under-prediction of $u^+(=u/u_\tau)$ is the over-prediction of $u_\tau(=\sqrt{\tau_w/\rho})$. When the velocity profiles in the dimensional form are compared, the Fluent-LS significantly over-predicts the near-wall velocity gradient, resulting in an over-prediction of τ_w and u_τ. This is consistent with the results shown in Fig. 1 where the friction coefficient is over-predicted by Fluent-LS.

Fig. 3 shows comparisons made with the experimental data of He [14] for an accelerating pipe flow with Reynolds number ramping from 7000 to 45,000 in 5 s. Predictions of Reynolds stress at four radial locations by TRANPIPE have previously been compared with the experimental data and predictions of Cotton et al. [20] in He et al. [15]. These are reproduced in Fig. 3a and b. In addition, the Fluent-LS and UDF-LS models are also used to simulate the same unsteady flow and results of which are shown in Fig. 3c and d, respectively.

It is seen that the prediction of UDF-LS of Reynolds stress distribution agrees very well with experimental data, which is consistent with the results of He [15] and Cotton [20]. As discussed in detail in He [14,15], the Reynolds stress remains frozen initially and later starts to respond first near the wall, then away from the wall. The initial period is called the *delay stage* which is smaller near the wall and increases with the distance away from the wall. For the first and the last radial locations (y = 1.9 mm and 21.4 mm), the UDF-LS predicts this delay to be ~1.2 s and ~3.4 s, respectively, which agree with the predictions of He [15] and Cotton [20]. The Fluent-LS, however, shows a faster response of turbulence across the radial locations, e.g., ~0.4 s and ~2.6 s at y = 1.9 mm and 21.4 mm, respectively.

Similar observations are made from the wall shear stress behaviour of the above transient flow, shown in Fig. 4. Wall shear stress response predicted by all three codes show the same characteristics of an initial overshoot followed by an undershoot and a recovery as discussed in He [14,15]. The TRANPIPE simulations of He [15] and the UDF-LS results obtained in this study show similar values of the time-scales for the wall shear stress overshoot, undershoot and its recovery. The Fluent-LS, however, predicts much lower values, i.e. much faster turbulence production in the near-wall region. This observation is consistent with that in Fig. 3.

4.2. Sensitivity of the LS model to small changes in its formulation

The second part of the study concerns the interpretation of the LS model. Three additional cases are considered to study the effects of using ε (instead of $\tilde{\varepsilon}$) in μ_t and Re_t as shown in Table 1. The values of wall shear stress of steady pipe flow at Re = 45,000 for the different implementations are shown in Fig. 5. Transient wall shear stress responses of these different cases are shown in Fig. 6 for the accelerating pipe flow ramping from Re = 7000 to 45,000 in 5 s.

It is observed that the use of different interpretations of the model has a significant impact on the prediction of the model. While Cases B to D under-predict the steady wall shear stress compared to UDF-LS (Case A), Fluent-LS over-predicts it. The prediction of the transient response of the wall shear stress shows the capability of the model in reproducing unsteady turbulence behaviours. Cases B to D show a much slower turbulent response to the imposed acceleration than that of the base case (UDF-LS). While the base case predicts that the wall shear stress starts to recover at ~1.8 s, Cases B and C predict this delay to be ~4 s and ~2.5 s, respectively. Case D predicts the slowest response, where the response of the wall shear stress does not reach the end of the delay period during the imposed acceleration period of 5 s. The Fluent-LS, on the other hand, predicts a much faster response with a delay of ~1.1 s.

These results show that although ε and $\tilde{\varepsilon}$ only differ in a very small region close to the wall, the choice of using either ε or $\tilde{\varepsilon}$ in μ_t and Re_t has a significant effect on the performance of the model in predicting both steady and unsteady flow behaviours. It is not surprising that the formulation using $\tilde{\varepsilon}$ works better than that using ε because the model was tuned using the former. Although theoretically speaking ε, not $\tilde{\varepsilon}$, should be used, there is no real significance in using either of them because of the empirical nature of

the damping functions. The difference can be absorbed by modifying the damping functions. For example, $\mu_t = \rho C_\mu f_\mu \frac{k^2}{\tilde{\varepsilon}}$ can be recast as $\mu_t = \rho C_\mu \left(f_\mu \frac{\varepsilon}{\tilde{\varepsilon}}\right)\frac{k^2}{\tilde{\varepsilon}}$, with a new damping function $f'_\mu = \left(f_\mu \frac{\varepsilon}{\tilde{\varepsilon}}\right)$. This way, ε indeed appears in the definition of μ_t .

5. Conclusions

An investigation has been carried out to study the sensitivity of the Launder–Sharma low-Reynolds number turbulence model to methods of implementation in CFD codes. A user-defined function (UDF) has been developed to implement the LS model to the commercial CFD code FLUENT. Its performance in predicting both steady and unsteady flows is compared with that of the inbuilt LS model in FLUENT and those implemented in several in-house codes previously reported in the literature. The UDFs developed have also been used to study the effect of using ε or $\tilde{\varepsilon}$ in the definition of μ_t and Re_t in the coding. The following conclusions have been drawn:

(1) With the formulation initially proposed in the original paper [4], the predictions of the presently implemented model (UDF-LS) and those of the 'in-house' codes reported in the literature agree well with each other. They closely reproduce steady and unsteady pipe flow experimental and DNS data. This confirms that the model is robust and insensitive to the numerical methods/coding used as long as the model formulation is the same.

(2) Theoretically speaking, ε rather than $\tilde{\varepsilon}$ should be used in the calculation of μ_t and Re_t, albeit the latter is used in the original paper. It has previously been assumed that this choice would have minor influence on results as they are the same everywhere in the flow field except for only a small region very close to the wall. However, our results show that the choice has significant effect on the predictions of the model and that the formulation proposed in the original paper (i.e. using $\tilde{\varepsilon}$) performs best when compared with experimental and DNS results.

(3) The FLUENT in-built LS model produces results that are significantly different from that of the LS implemented in FLUENT using UDF in the present study and those of results published in the literature using 'in-house' codes. The Fluent-LS model predictions compare rather badly with experimental and DNS data. This is likely to be associated with the formulation chosen to be used in the code rather than the numerical methods used as demonstrated through comparisons between the simulations of Fluent-LS and UDF-LS, which are based on the same numerical/coding framework.

Appendix A. Supplementary data

Supplementary data associated with this article can be found, in the online version, at http://dx.doi.org/10.1016/j.compfluid.2013.02.020.

References

[1] Launder BE, Spalding DB. The numerical computation of turbulent flows. Comput Methods Appl Mech Eng. 1974;3:269–89.
[2] Jones WP, Launder BE. The prediction of laminarization with a two-equation model of turbulence. Int J Heat Mass Transfer 1972;15:301–14.
[3] Jones WP, Launder BE. The calculation of low-Reynolds-number phenomena with a two-equation model of turbulence. Int J Heat Mass Transfer 1973;16:1119–30.
[4] Launder BE, Sharma BL. Application of the energy-dissipation of turbulence to calculation of low near a spinning disc. Lett Heat Mass Transfer 1974;1:131–8.
[5] Patel VC, Rodi W, Scheuerer G. Turbulence models for near-wall and low-Reynolds number flows – a review. AIAA 1985;23:1308–19.
[6] Betts PL, Dafa'Alla AA. Turbulent buoyant air flow in a tall rectangular cavity. In: Significant questions in buoyancy affected enclosure or cavity flows, Prec. ASME Winter Annual Meeting, vol. 60; 1986.
[7] Hrenya CM, Bolio EJ, Chakrabarti D, Sinclair JL. Comparison of low Reynolds number k–ε turbulence models in predicting fully developed pipe flow. Chem Eng Sci 1995;50:1923–41.
[8] Hrenya C, Miller S, Mallo T, Sinclair J. Comparison of low-Reynolds number k–ε models in predicting heat transfer rates for pipe flow. Int J Heat Mass Transfer 1998;41:1543–7.
[9] Thakre SS, Joshi JB. CFD modeling of heat transfer in turbulent pipe flows. AIChE J 2000;46:1798–812.
[10] Cotton MA, Jackson JD. Vertical tube air flows in the turbulent mixed convection regime calculated using a low-Reynolds number k–ε model. Int J Heat Mass Transfer 1990;33:275–86.
[11] Kim WS, He S, Jackson JD. Assessment by comparison with DNS data of turbulence models used in simulations of mixed convection. Int J Heat Mass Transfer 2008;51:1293–312.
[12] He S, Jiang P, Xu Y, Shi R, Kim WS, Jackson JD. A computational study of convection heat transfer to CO_2 at supercritical pressures in a vertical mini tube. Int J Therm Sci 2005;44:521–30.
[13] Jackson JD, Büyükalaca O, He S. Heat transfer in a pipe under conditions of transient turbulent flow. Int J Heat Fluid Flow 1999;20:115–27.
[14] He S. On transient turbulent pipe flow. Doctoral thesis. UK: University of Manchester; 1992.
[15] He S, Ariyaratne C, Vardy A. A computational study of wall friction and turbulence dynamics in accelerating pipe flows. Comput Fluids 2008;37:674–89.
[16] He S, Ariyaratne C. Wall shear stress in the early stages of unsteady turbulent pipe flow. J Hydraul Eng 2011;137:606–10.
[17] Ariyaratne C, He S, Vardy A. Wall friction and turbulence dynamics in decelerating pipe flows. J Hydraul Res 2010;48:810–21.
[18] Ismael JO, Cotton MA. Calculations of wall shear stress in harmonically oscillated turbulent pipe flow using a low-Reynolds number k–ε model. J Fluids Eng 1996;118:189–94.
[19] Cotton MA. Resonant responses in periodic turbulent flows: computations using a k–ε eddy viscosity model. J Hydraul Res 2007;45:54–61.
[20] Cotton MA, Guy AW, Launder BE. Second-moment modelling of periodic and transient pipe flow. In: Proceedings of the 11th symposium on turbulent shear flows, Grenoble; 1997. p. 14.6–11.
[21] Cotton MA, Craft TJ, Guy AW, Launder BE. On modelling periodic motion with turbulent closures. Flow Turbul Combust 2001;67:143–58.
[22] Wang SJ, Majumdar AS. A comparitive study of five low-Reynolds number k–ε models for impingement heat transfer. Appl Therm Eng 2005;25:31–44.
[23] Du Z, Lin W, Gu A. Numerical investigation of cooling heat transfer to supercritical CO_2 in a horizontal circular tube. J Supercrit Fluids 2010;55:116–21.
[24] Jagadeesh P, Murali K. Application of low-Re turbulence models for flow simulations past underwater vehicle hull forms. J Naval Architect Marine Eng 2005;1:41–54.
[25] Iaccarino G. Predictions of a turbulent separated flow using commercial CFD codes. J Fluids Eng 2001;123:819–28.
[26] Eggels JGM, Unger F, Weiss MH, Westerweel J, Adrian RJ, Friedrich R, et al. Fully developed turbulent pipe flow: a comparison between direct numerical simulation and experiment. J Fluid Mech 1994;268:175–209.
[27] Boersma BJ. Direct numerical simulation of turbulent pipe flow up to a Reynolds number of 61,000. J Phys: Conf Series 2011;318:042045.
[28] Wu X, Moin P. A direct numerical simulation study on the mean velocity characteristics in turbulent pipe flow. J Fluid Mech 2008;608:81–112.